BMC Oral Health

RESEARCH

Open Access

Evaluation of trabecular bone microstructure and cortical morphology using cone-beam and micro-CT images: impact of tube voltage setting

Oğuzhan Baydar[1*], Erinc Onem[2], Ali Mert[3] and B Guniz Baksi[2]

Abstract

Objective To evaluate the effect of various tube voltage (kV) settings on the accuracy of cone-beam computed tomography (CBCT) images in measuring trabecular microstructure and cortical morphology, using micro-CT (μCT) as the reference.

Methods Ten bone samples of sheep mandibles were scanned using both μCT and CBCT at three different tube voltage settings (80, 85, and 90 kV). Identical regions of interest (ROIs) on trabecular and cortical bones were analyzed in all images. Measurements of trabecular microstructure included bone volume fraction (BV/TV), trabecular thickness (Tb.Th) and space (Tb.Sp), while thickness (Ct.Th) and area (Ct.Ar) of cortical bone were measured to determine cortical morphology. Measurements were compared using paired t-test, while agreement between measurements of two modalities was assessed using Bland–Altman analysis. One-way ANOVA was used to determine differences in measurements of CBCT images at different kVs ($p < 0.01$).

Results Compared to μCT, CBCT overestimated trabecular parameters and Ct.Th but underestimated Ct.Ar, with high agreement observed between the methods. Significant differences were found for all measurements except BV/TV and Ct.Ar at all kVs. No differences were observed between CBCT measurements at different tube potentials.

Conclusion The tube voltage of CBCT has minimal impact on the measurement accuracy of most microstructural parameters. BV/TV and Ct.Ar measurements may be particularly preferred for bone evaluations using CBCT images.

Keywords Bone microarchitecture, Tube voltage, CBCT, Micro-CT

Introduction

Alveolar bone is one of the crucial elements that significantly contribute to the primary and long-term stability of dental implants [1]. It was well acknowledged that alveolar bone has a complex structure that cannot be simply assessed by bone density. Therefore, evaluation of qualitative and quantitative characteristics of bone has been recommended for constitution of primary stability and osseointegration of dental implants [2–5]. Planning dental implant therapy and thread design requires accurate clinical assessment of bone structure

*Correspondence:
Oğuzhan Baydar
oguzhan_baydar_94@hotmail.com
[1] Faculty of Dentistry, Department of Oral and Maxillofacial Radiology, Eskisehir Osmangazi University, Eskişehir, Turkey
[2] School of Dentistry, Department of Oral and Maxillofacial Radiology, Ege University, Izmir, Turkey
[3] Faculty of Engineering and Architecture, Department of Engineering Sciences, Izmir Katip Celebi University, Izmir, Turkey

and mechanical properties. The evaluation of trabecular bone microstructure and cortical bone morphology is essential for the long-term success of dental implants, as both types of bone are in direct contact with the implant surface. Furthermore, microstructural analysis of alveolar bone is important for the assessment of peri-implant bone tissue and bone volume following bone grafting as well as the effective diagnosis of peri-implantitis for considering early treatment options. Micro-architectural characteristics of trabecular and cortical bone have been thoroughly investigated using bone biopsies, combined with calculation of morphometric parameters. However, due to its irreversible nature and high acquisition costs, histomorphometry has been replaced by reproducible radiomorphometric methods for the evaluation of bone microstructure. Micro-CT (μCT) is recognized as the gold standard for evaluating bone microstructure, as it offers both morphometric features and densitometric parameters of trabecular and cortical bone. [6] However, its in vivo use is not convenient due to the small scanning area [7–9]. Therefore, several studies recommend using high-resolution cone-beam computed tomography (CBCT) for quantifying bone microstructure surrounding dental implants. While intraoral radiographs are still regarded as the main tool for postoperative implant monitoring, current guidelines for the clinical use of CBCT in implant dentistry state that assessment of three-dimensional bone healing, including morphological, volumetric, and trabecular remodeling is mandatory [10].

Numerous studies assessing the microstructure of alveolar bones have compared the performance of CBCT with either μCT or multidetector computed tomography (MDCT) [11–13]. There are also many studies examining the effect of various exposure parameters on the performance of CBCT for the determination of bone microstructure [14–17]. However, the impact of exposure parameters on microstructure measurements had only been assessed in a single study [18]. The authors have stated that "*results of bone structure analysis would be clinically applicable only if the measured values are independent of changes in exposure parameters.*" [18]. The X-ray tube potential is the most significant exposure parameter influencing diagnostic data in CBCT. However, there is a lack of knowledge concerning the potential impact of tube voltage on CBCT images used to evaluate bone microstructure. In addition to the fact that the effect of tube voltage has not been studied, the majority of the aforementioned studies have only included the microstructure of trabecular bone examinations, but studies assessing cortical bone morphology were rare [19].

Therefore, the aim of this study was to evaluate the effect of different tube voltage settings on the accuracy of radiomorphometric measurements of trabecular and cortical bone using CBCT images and to compare them with gold-standard measurements of μCT images. The null hypothesis is that the change in tube potential of CBCT would not alter radiomorphometric measurements.

Materials and methods

Ethical approval and sample size calculations

The study protocol was approved by the University's Local Ethics Committee for Animal Experiments (protocol no: 2020–034, approval date: February 26, 2020). The study adhered to ethical guidelines for the use of animal tissues, and no animals were sacrificed specifically for the purposes of this research. Considering the smallest difference between the groups, the standard deviation, and the number of repetitions, the number of necessary measurements was calculated using Cochran's sample size formula with a confidence level of 99% and 0.06 margin of error using a pre-determined variance value ($\sigma = 0.0144$) from a previous similar study [5]. Even though the result of the calculation was a minimum of 27, thirty measurements were done on each set of images to increase statistical power and reliability.

Preparation of bone samples

Sheep mandibles (*Ovis aries domesticus*) were used in this study due to legal restrictions on obtaining dry human cadaver skulls. Fresh skulls were procured from a certified ovine producer; no animals were sacrificed for this investigation. To ensure standardization, mid-sized mandibles (14–18 cm in length) from carcasses of *Ovis aries domesticus* weighing 20 to 30 kg were selected.

Ten bone samples, including both trabecular and cortical bone, were obtained from the right and left posterior regions of five sheep mandibles using a bone saw and cleared of residual soft tissues (Fig. 1). Similar to the method used by He et al., the bone samples of 40 × 80x20 mm in size were covered with gauze soaked in saline solution and stored in a −20°C freezer until further processing. Before imaging, all samples were allowed to defrost at room temperature for approximately 6 to 8 h. [19] In order to provide a reference for measurements and to ensure the measurement of identical regions of interest (ROIs) with both imaging methods, a horizontal guide groove was drilled on the facial surface of all bone samples from one end to the other using a round 1.4 mm diamond bur (Dentex Dental, *New Taipei City, Taiwan*). To simulate soft tissue, the samples were covered with pink wax and then supported with Styrofoam boards for stabilization and mounted onto a silicone holder to prevent micromovements during image acquisition (Fig. 1). [19] Finally, the samples were scanned with both imaging methods with their occlusal plane parallel to the floor,

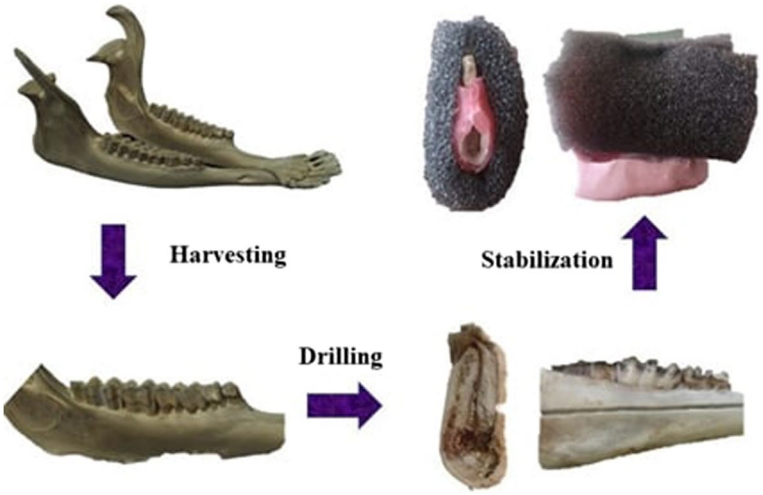

Fig. 1 Image of sheep mandibles prior to CBCT and micro-CT imaging demonstrating horizontal guide groove, pink wax for soft-tissue simulation, and styrofoam boards mounted onto a silicon holder for stabilization

corresponding to the orientation of a human jaw during scanning for implant planning (Fig. 1).

Imaging

μCT images of the bone samples were obtained using the μCT50 (SCANCO Medical, *Basserdorf, Switzerland)*, at 90 kV and 155 μA, with a voxel size of 20 μm and an exposure time of 15 min. For CBCT scanning, bone samples were located in the center of the 4×4 cm FOV of the 3D Accuitomo 170 CBCT device (J. Morita, *Kyoto, Japan*) and scanned three times with exposure parameters of 4 mA, 30.8 s, and 80 μm isotropic voxel size using three tube voltage settings (80, 85, and 90 kV) respectively.

A total of 40 images of (10 μCT; 30 CBCT) ten bone samples were obtained in DICOM file format and converted to 8-bit files for further processing with an image analysis software.

Image processing and analysis

All measurements were performed by three oral and maxillofacial radiologists on sagittal slices using the same flat panel monitor (Philips 275E1S, Philips Electronics Nederland B.V. *Eindhoven, The Netherlands*) in a semi-dark room. The morphometric measurements were done using Java-based image processing software (ImageJ-National Institutes of Health, *Bethesda, Maryland, USA*). In order to ensure the measurement of identical ROIs and accordingly minimize the measurement errors among observers, the long axis of all bone images was aligned so that the occlusal plane was perpendicular to the floor. For further standardization of the measurements, the depth of the reference groove and the thickness of the soft-tissue material were used as a guide in order to select the corresponding slices. Then, all images were blurred with a Gaussian filter ($\sigma=2$) to minimize noise and eliminate artifacts. Three interdental bone regions containing both trabecular and cortical bone were selected on the image of each bone sample. Thus, a total of 120 ROIs (30 μCT, 90 CBCT) containing both trabecular and cortical bone structures were used for measurements.

Morphometric measurements

For the measurement of trabecular bone parameters, a 5×5 mm square-shaped ROI was cropped 5 mm lingual to the deepest point of the reference groove from the interdental spaces of three neighboring posterior teeth (Fig. 2a). Ten consecutive slices from μCT and forty from CBCT images were used for measurements. Since the voxel size of μCT (20 μm) is one-fourth of CBCT (80 μm), four times more slices were used for CBCT to ensure that the measurements were done on matching ROIs for both image types. Before all measurements, all ROIs of both μCT and CBCT images were segmented to create binary images using the same software. Measurements of trabecular microstructure included bone volume fraction (BV/TV), trabecular thickness (Tb.Th) and space (Tb.Sp), while thickness (Ct.Th) and area (Ct.Ar) of cortical bone were measured to determine cortical morphology. These measurements were done using the *BoneJ* and *Area Fraction* plugins of ImageJ software (Table 1). While some of these morphometric parameters were linear measurements (Tb.Th, Tb.Sp and Ct.Th), others were either area (Ct.Ar) or proportional (BV/TV) measurements determining the structure of selected bone. The definition of the measurement parameters as well as the measurement steps using can be followed in Table 1.

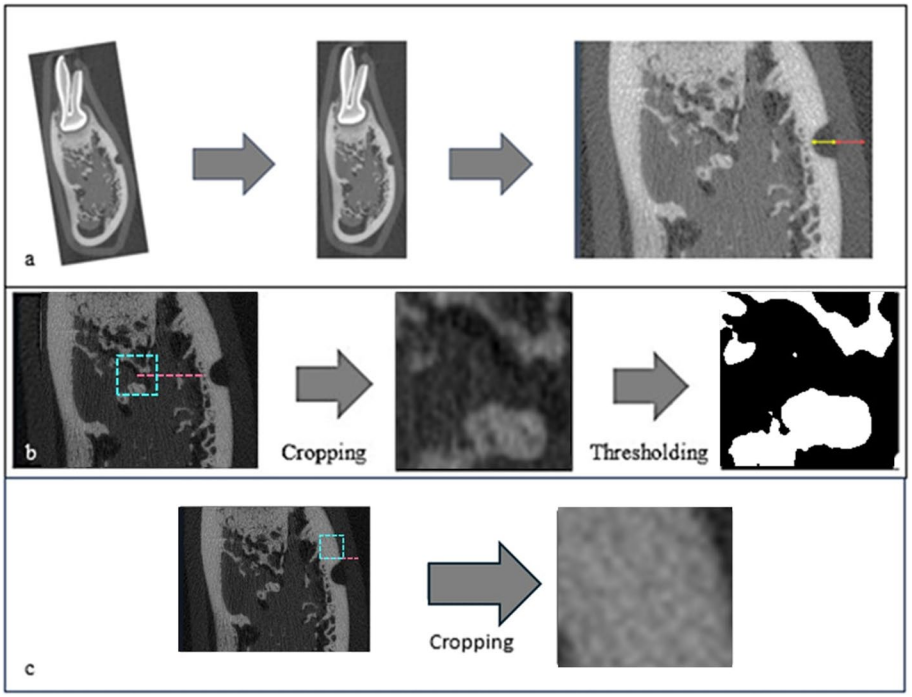

Fig. 2 Pre-processing of the image sections before morphometric measurements. **a** alignment of image sections, and their subsequent matching (**b**) creation of regions of interest (ROIs) for trabecular measurements and binarization (**c**) Selection of ROIs for cortical measurements

Table 1 Definitions and measurement steps of radiomorphometric parameters using *ImageJ* software

Parameters	Abbreviation	Definition	Measurement steps
Bone volume fraction	BV/TV	The proportion of bone volume to the total volume within the region of interest (ROI)	Binarized ROI was analyzed using the *Area Fraction* plugin
Trabecular thickness	Tb.Th	The mean thickness of individual trabeculae within the selected region	Binarized ROI was analyzed using the *Thickness* feature of the BoneJ plugin
Trabecular separation	Tb.Sp	The mean distance between adjacent trabeculae in the selected region	Binarized ROI was analyzed using the *Thickness* feature of the BoneJ plugin
Cortical area	Ct.Ar	The area of the cortical bone in the selected region	Measured using the '*Slice Geometry*' command in BoneJ, focusing on the upper border of the reference groove
Cortical thickness	Ct.Th	The average thickness of the cortical bone in the analyzed region	Measured using the '*Slice Geometry*' command of BoneJ after aligning the cortical bone axis perpendicular to the floor

Abbreviations: *BV/TV* Bone Volume Fraction, *Tb.Th* Trabecular Thickness, *Tb.Sp* Trabecular Separation, *Ct.Th* Cortical Thickness, *Ct.Ar* Cortical Area

For measurements of trabecular bone parameters, the method of Panmakiate et al. was used, and the selected ROI was binarized using the '*Image > Adjust > Threshold*' commands to extract the trabecular bone in each ROI (Fig. 2b) [20]. Thereafter, for all ROIs, three trabecular bone measurements were done including bone volume fraction (BV/TV), trabecular thickness (Tb.Th) and trabecular separation (Tb.Sp) using the *BoneJ* plug-in of the software [21]. Since ImageJ can only analyze foreground black pixels in a binary image, BV/TV and Tb.Th were calculated using binary images where bone regions were represented by black pixels. Conversely, to measure Tb.Sp, binary images were used where black pixels represented bone marrow. The BV/TV of trabecular ROIs was determined using the Area Fraction plugin, which calculates the percentage of pixels representing trabecular bone relative to the total bone volume. Tb.Th and Tb.Sp were measured using the Thickness feature of the *BoneJ* plugin in ImageJ for both µCT and CBCT.

In order to minimize the margin of measurement errors, the long axes of the cortical bone in the sagittal images were aligned perpendicular to the floor using the

'Plugins > BoneJ > Moments of Inertia' commands before the measurement of cortical bone parameters. Cortical area (Ct.Ar) and thickness (Ct.Th) were then measured on 120 ROIs using the '*Slice Geometry'* command of the software corresponding to the upper border of the reference groove (Fig. 2c) [21, 22].

Statistical analysis

Statistical analysis was performed using the IBM SPSS Statistics 22 package (SPSS version 22.0, SPSS Inc. *Chicago, IL, USA*). The mean and standard deviations (SD) of all measurements were calculated for µCT and CBCT images at 3 different tube voltage settings. Differences between the CBCT measurements obtained with three different tube voltages were compared using a one-way analysis of variance (ANOVA). The normality of the data was evaluated using the Kolmogorov–Smirnov test. After confirmation of the normal distribution of the data, a paired t-test was used for the pairwise comparisons of measurements from CBCT and µCT images. The significance level for all statistical tests was set as p = 0.01.

The level of agreement between the measurements of CBCT and µCT, was determined using Bland–Altman plots. To assess inter-observer reliability, each of the 10 randomly selected interdental regions was measured twice at two-week intervals on both µCT and CBCT images for all tube voltage settings. The reliability was evaluated using the inter-class correlation coefficient (ICC), following the grading scale proposed by Koo and Li (2016) [23].

Results

The means and standard deviations (SDs) of both trabecular and cortical bone measurements are presented in Table 2. In general, all the trabecular bone measurements were considerably similar at all three kV settings for CBCT images and identical for BV/TV (Table 2).

The BV/TV, Tb.Th and Tb.Sp measured on CBCT images were relatively higher than those of µCT measurements. While Tb.Th measurements showed a minor increasing trend as tube voltage raised from 80 to 90, measurements of Tb.Sp showed a slight decrease when kV was increased from 85 to 90 (Table 2).

The cortical area (Ct.Ar) measurements were lower for CBCT images obtained at 80 and 85 kV, but higher at 90 kV as compared to µCT measurements. Cortical thickness (Ct.Th) as measured on CBCT images was higher than µCT measurements at all tube voltage settings (Table 2).

No difference was found between µCT and CBCT measurements obtained with 3 different tube voltage settings for BV/TV and Ct.Ar ($p > 0.01$, Table 3). However, the differences between µCT and CBCT for Tb.Th, Tb.Sp and Ct.Th measurements were significant for all kVs ($p < 0.01$, Table 2). Similarly, no significant difference was obtained among the measurements of CBCT images generated at 80, 85, and 90 kV for bone parameters measured in this study (Table 3).

The Bland–Altman plots revealed that CBCT measurements obtained with different tube voltages for all morphometric measurements were around the mean and within the 95% limits of agreement (Table 4).

Measurements including BV/TV, Tb.Th, and Tb.Sp for trabecular bone as well as Ct.Ar measurement for cortical bone plots showed a similar distribution throughout the graph. However, there was an upward trend for Ct.Th measurements in Bland–Altman plots indicating that as the mean difference between measurements of the two methods increased, the bias between the imaging modalities increased as well (Fig. 3).

Table 2 Measurements of trabecular and cortical bone on CBCT images acquired at three (80,85,90) tube voltage settings

	µCT	CBCT		
	90 kV	80 kV	85 kV	90 kV
	Mean ± SD	Mean ± SD	Mean ± SD	Mean ± SD
Trabecular measurements				
BV/TV (%)	40 ± 13	42 ± 13	42 ± 14	42 ± 12
Tb.Th (mm)	0.65 ± 0.35	1.06 ± 0.36	1.07 ± 0.34	1.08 ± 0.37
Tb.Sp (mm)	0.94 ± 0.57	1.35 ± 0.55	1.45 ± 0.65	1.42 ± 0.58
Cortical measurements				
Ct.Ar (mm^2)	9425.53 ± 2011.38	9401.90 ± 2042.81	9407.17 ± 2033.61	9440.63 ± 2027.65
Ct.Th (mm)	1.71 ± 0.47	2.13 ± 0.48	2.16 ± 0.49	2.15 ± 0.47

µCT micro-CT, *CBCT* cone beam computer tomography, *SD* standard deviation, *BV/TV* bone volume fraction, *Tb.Th* trabecular thickness, *Tb.Sp* trabecular separation, *Ct.Ar* cortical area, *Ct.Th* cortical thickness

Table 3 Comparison of measurements from µCT and CBCT images acquired at three different voltage settings

	Trabecular measurements			Cortical measurements	
	BV/TV (%)	Tb.Th (mm)	Tb.Sp (mm)	Ct.Ar (mm^2)	Ct.Th (mm)
µCT—$CBCT_{80}$[a]	0.3111	< 0.0001*	< 0.0001*	0.9626	< 0.0001*
µCT—$CBCT_{85}$[a]	0.2110	< 0.0001*	< 0.0001*	0.7302	< 0.0001*
µCT—$CBCT_{90}$[a]	0.2272	< 0.0001*	< 0.0001*	0.8372	< 0.0001*
$CBCT_{80–85–90}$[b]	0.976	0.972	0.793	0.998	0.970

µCT micro-CT, *CBCT* cone beam computer tomography; volume, *BV/TV* bone volume fraction, *Tb.Th* trabecular thickness, *Tb.Sp* trabecular separation, *Ct.Ar* cortical area, *Ct.Th* cortical thickness

* Statistical significance ($p < 0.01$)

[a] Paired T-tests

[b] ANOVA

Table 4 Mean differences and 95% limits of agreement between measurements obtained with µCT and CBCT images at different tube voltage settings

	Mean difference ± standard deviation	Limits of agreement (95%)		*p*-value
		Lower	Upper	
Trabecular measurements				
BV/TV (%)				
µCT-$CBCT_{80}$	−2.16 ± 11.51	−24.72	20.40	0.3111
µCT-$CBCT_{85}$	−2.83 ± 12.13	−26.60	20.40	0.2110
µCT-$CBCT_{90}$	−2.33 ± 9.91	−21.75	17.09	0.2272
Tb.Th (mm)				
µCT-$CBCT_{80}$	−0.41 ± 0.05	−0.93	0.11	< 0.0001*
µCT-$CBCT_{85}$	−0.41 ± 0.05	−0.94	0.11	< 0.0001*
µCT-$CBCT_{90}$	−0.43 ± 0.05	−0.93	0.07	< 0.0001*
Tb.Sp (mm)				
µCT-$CBCT_{80}$	−0.40 ± 0.12	−1.65	0.83	< 0.0001*
µCT-$CBCT_{85}$	−0.51 ± 0.11	−1.66	0.64	< 0.0001*
µCT-$CBCT_{90}$	−0.43 ± 0.11	−1.65	0.69	< 0.0001*
Cortical measurements				
Ct.Ar (mm^2)				
µCT-$CBCT_{80}$	−5.26 ± 111.23	−1199	1188	0.9626
µCT-$CBCT_{85}$	−38.73 ± 111.22	−1232.74	1155.27	0.7302
µCT-$CBCT_{90}$	−23.63 ± 113.98	−1247.33	1200.06	0.8372
Ct.Th (mm)				
µCT-$CBCT_{80}$	−0.42 ± 0.07	−1.16	0.31	< 0.0001*
µCT-$CBCT_{85}$	−0.45 ± 0.08	−1.26	0.35	< 0.0001*
µCT-$CBCT_{90}$	−0.44 ± 0.07	−1.21	0.33	< 0.0001*

µCT micro-CT, *CBCT* cone beam computer tomography, *SD* standard deviation, *BV/TV* bone volume fraction, *Tb.Th* trabecular thickness, *Tb.Sp* trabecular separation, *Ct.Ar* cortical area, *Ct.Th* cortical thickness

* Statistical significance ($p < 0.01$)

Interobserver reliability was excellent, ranging from 0.91 to 0.97 for µCT and 0.92 to 0.97 for CBCT. ICC scores for CBCT were generally greater than or equal to µCT scores for all measurements (Table 5).

Discussion

The amount and quality of alveolar bone are of paramount importance for implant planning, evaluation of regeneration of intra-bony defects, orthodontic tooth movement, as well as evaluation of the effect of different types of medications on bone [2, 3, 24]. Many studies have evaluated the effect of tube current as well as various FOV & voxel sizes on the micromorphometric measurements of trabecular bone. [16, 18, 25] However, the effect of tube voltage on micromorphometric measurements using CBCT has been previously evaluated in conjunction with milliampere, but not alone and exclusively for trabecular bone [18].

The optimal kV value for a specific diagnostic task has not yet been determined; however, a recent study on dental CBCT scanners found that the maximum tube voltage, ranging from 70 to 90 kV, provided the optimum balance between technical image quality, radiation dose, and reduced noise. [26] Tube potentials used in this study were selected based on their widespread use in clinical practice and according to the recommendations regarding the optimum clinical assessment of bone structures for implant planning, ensuring optimal image quality while maximizing contrast of the image data. [26–28].

In contemporary bone research, a variety of animal models are employed due to challenges in acquiring desiccated human mandible specimens and adhering to ethical guidelines [29–31]. Sheep and bovine mandibles are commonly favored models, particularly in radiomorphometric studies, contingent upon gantry size. At the microscopic level, sheep present a mainly primary bone structure in contrast to the predominantly secondary one in humans [32]. Although sheep lack secondary osteons, they were generally proved to be a good model mimicking human bone biology and healing, plus biomechanical behavior observed in human mandibles [32–36]. Accordingly, sheep mandibles were used in the present study due to their similarity to human mandibular bone tissue

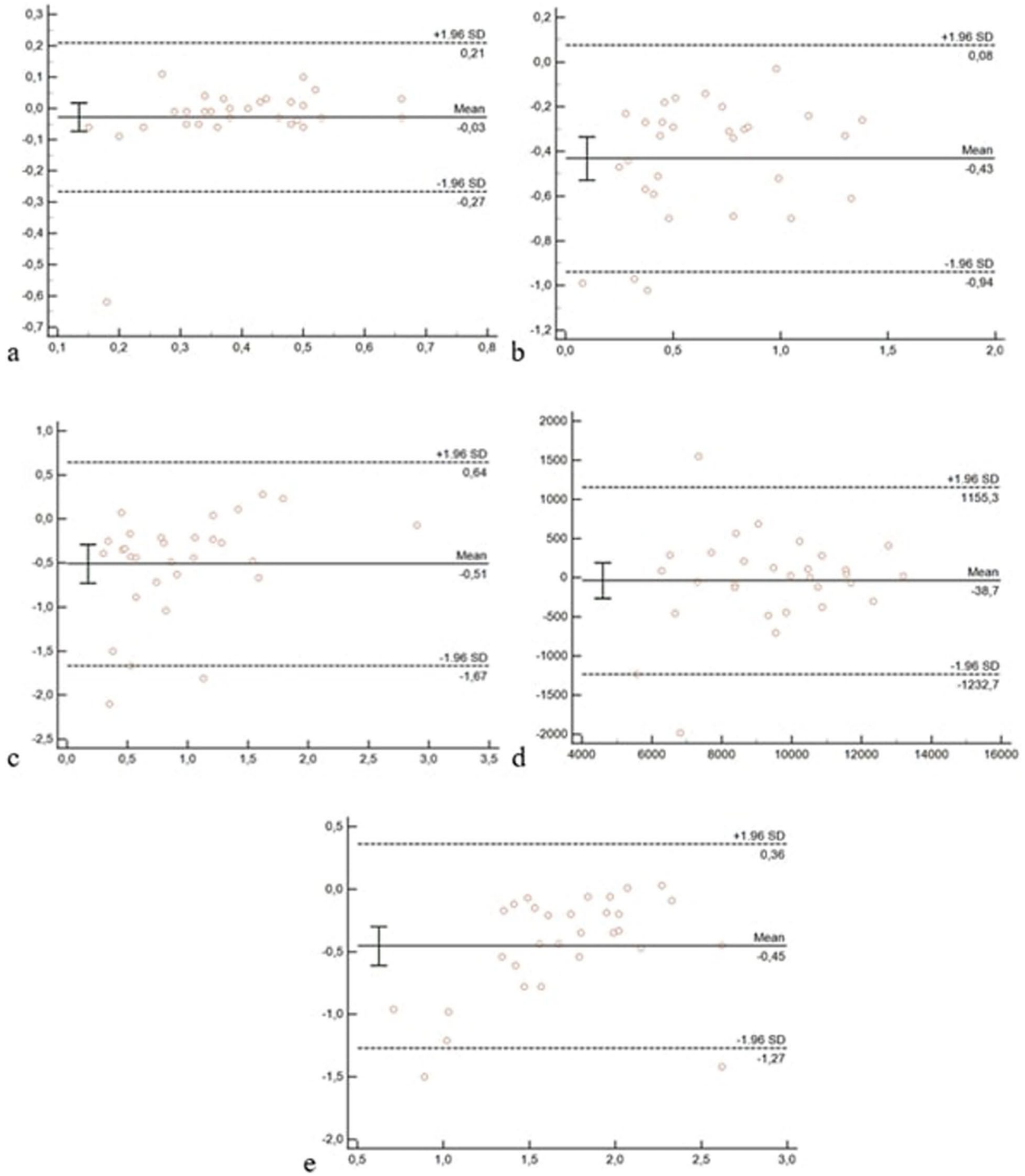

Fig. 3 Representative Bland–Altman plots demonstrating the agreement between µCT and CBCT at the kV settings showing the highest agreement for trabecular bone parameters: BV/TV at 85 kV (**a**); Tb.Th at 90 kV (**b**); Tb.Sp at 85 kV (**c**); and cortical bone parameters Ct.Ar (**d**) and Ct. Th (**e**) at 85 kV. X-axis of the graphs represents the mean of µCT and CBCT measurements, while y-axis represents the difference in measurements of µCT and CBCT at the given tube voltage. The solid line parallel to the x-axis indicates the mean difference, the line parallel to the y-axis represents the 95% confidence interval for the mean difference, and the dashed lines indicate the lower and upper limits of agreement within ± 95% confidence intervals. Abbreviations: µCT, micro-CT; CBCT, cone beam computed tomography; SD, standard deviation; BV/TV, bone volume fraction; Tb.Th, trabecular thickness; Tb.Sp, trabecular separation; Ct.Ar, cortical area; Ct.Th, cortical thickness

Table 5 Intra-class correlation coefficients (ICC) of μCT and CBCT measurements

	ICC			
	μCT	CBCT		
		80 kV	85 kV	90 kV
Trabecular measurements				
BV/TV	0.97	0.96	0.96	0.95
Tb.Th	0.92	0.93	0.94	0.92
Tb.Sp	0.91	0.92	0.92	0.93
Cortical measurements				
Ct.Ar	0.96	0.97	0.96	0.97
Ct.Th	0.95	0.96	0.96	0.95

ICC Intra-class correlation coefficients, *μCT* micro-CT, *CBCT* cone beam computer tomography, *BV/TV* bone volume fraction, *Tb.Th* trabecular thickness, *Tb.Sp* trabecular separation, *Ct.Ar* cortical area, *Ct.Th* cortical thickness

and to their particular convenience in micro-CT exposures. [29, 30].

The findings of the present study revealed that CBCT measurements overestimated all of the measured parameters but underestimated Ct.Ar measurements as compared to μCT at all tube voltage settings. This may be due to the lower resolution of CBCT images since it has been already proved that decreasing the resolution of μCT images similarly resulted in overestimation of BV/TV, Tb.Sp and Tb.Th measurements [37]. Bone trabeculae thinner than image resolution were smeared out, resulting in an increase in Tb.Th and consequently in Tb.Sp. It is well known that the spatial resolution of images has been crucial for correct structural analysis of bone microstructure and particularly for measurements of Tb.Th, which has been proved to require high resolution for accurate measurements [37]. The results obtained for Ct.Th measurements in this study support this assumption as well; however, more studies evaluating the cortical bone are needed to justify its validity.

A significant difference was obtained between measurements of μCT and CBCT, except for BV/TV and Ct.Ar for all tube voltage settings. BV/TV, expressed as the trabecular bone volume (BV) relative to tissue volume (TV) in percentage, is a key indicator of bone gain and loss and is widely used to evaluate pathologies that affect bone turnover. Recognized as one of the most critical histomorphometric parameters, BV/TV also has a strong association with mechanical properties, underscoring its importance in assessing structural integrity [38]. Our results demonstrated that the measurements of BV/TV were overestimated in CBCT; however, in accordance with our null hypothesis, not affected by change in tube voltage. Moreover, Bland–Altman plots revealed that differences between CBCT and μCT were minimal (−2.00/μm), suggesting a strong agreement between measurements of these two imaging methods for BV/TV. The negative bias value in the Bland–Altman plot indicates the higher measurement values of CBCT. However, the small range of confidence interval indicating high stability between the measurements of two imaging modalities (min 0.17 / max −0.27) for all kVs, supports the agreement of BV/TV measurements of CBCT and μCT. These results indicate that regardless of the change in tube voltage BV/TV measured on CBCT images can be a reliable parameter for the determination of trabecular microstructure, and CBCT can be safely used as an alternative to μCT. This finding is in accordance with previous reports demonstrating the accuracy of BV/TV obtained from CBCT in evaluating the microstructure of trabecular bone [5]. However, it should be remembered that the present study used the smallest FOV and voxel size (0.08 mm) during CBCT scanning in order to obtain high-resolution images and that the results might vary depending on the CBCT device and other exposure parameters. Another crucial factor is that the patient's movement largely impairs image quality during CBCT scan. The ex vivo nature of this study might have contributed to the quality of the CBCT images since they did not suffer from movement artifacts.

It has been well acknowledged that gray scale values measured by CBCT are not a reliable indicator of bone density, and trabecular bone microstructure should be considered as part of the pre-surgical bone evaluation before dental implant treatment [39]. Trabecular bone microstructure signifies bone strength; aids bone healing and implant retention and accordingly affects the long-term success of dental implants. In order to evaluate bone quality and to choose the most optimal surgical protocol prior to dental implant treatment, trabecular microstructural assessment is mandatory for elucidating bone strength [40]. The most commonly recommended microstructural parameters for the determination of bone strength include Tb.Th and Tb,Sp, which are also crucial determinants of bone fragility [41]. Many studies have revealed a strong agreement between measurements of μCT and CBCT for Tb.Th and Tb.Sp. According to our results, measurements of Tb.Th and Tb.Sp were significantly higher in CBCT as compared to μCT. However, the Tb.Th and Tb.Sp measurements of CBCT images were about two-thirds higher than those on the μCT measurements for all tube voltages. These findings are consistent with the results of studies comparing various imaging modalities for the assessment of bone structure. [42, 43] The discrepancy between measurements of two imaging systems is directly linked to the partial volume artefacts leading to volume overestimation and therefore higher CBCT measurements [44]. Another

reason may be the larger voxel size of the CBCT images. It has been demonstrated that thin trabecula is poorly detected in low-resolution images, causing an increase in Tb.Th and Tb.Sp measurements [45]. Nevertheless, it should be remembered that spatial resolution, indicated as voxel size is not the single factor contributing to the image quality of an imaging system. Contrast-to-noise ratio (CNR) also plays a significant role on the image quality and the delineation of delicate trabeculae, thus affecting measurement accuracy. It has been advocated that with sufficiently high CNR, thin trabeculae can be depicted even when the trabecular thickness exceeds the nominal voxel size [46].

Ct.Ar measurements are considered to be of critical importance for the determination of osteoporosis, as well as its role in the distribution of lateral and oblique forces reaching the implant surface. In addition, it has been used for evaluating the treatment efficacy of various anti-resorptive drugs. Our results revealed although Ct.Ar measurements obtained with CBCT were lower than µCT, no significant difference could be found between measurements of the two imaging modalities. In fact, Bland–Altman plots demonstrated strong agreement supporting our null hypothesis that morphometric measurements were not affected from change in tube voltage. Contrary to the measurements obtained for Ct.Ar, our results demonstrated higher Ct.Th values for CBCT as compared to that of µCT. In addition, the difference between the measurements of the two methods was significant for Ct.Th measurements. It has been established that CBCT images have a higher background noise than µCT, which is produced by the reconstruction algorithms used to create the CBCT image as well as higher amount of scatter [47]. Due to the combined effects of lower signal-to-noise ratio, reduced contrast, beam-hardening, and edge-aliasing artifacts of CBCT images, discrepancies arise, particularly in thickness measurements. This is an expected finding since it has been proved that maximum deviations are observed at the measurements that involve margins and edges as in Ct.Th measurements [48]. Greater voxel size of the CBCT images has further contributed to the differences in Ct.Th measurements of the two imaging methods because measurement precision is closely related to voxel size [49].

Ct.Th has been identified as one of the critical parameters influencing primary stability as well as micromotion (displacement between implant and bone) and the success of osseointegration [50]. Given that the radiation exposure to biological tissues should be as low as possible, clinical CBCT images would contain more noise and have lower resolution and accordingly may cause higher deviation in thickness measurements. Therefore, it is advisable to keep a greater margin of safety for bone thickness measurements during implant planning with CBCT images.

The increase in tube voltage is assumed to influence the assessment of bone architecture, as both the signal-to-noise ratio and scatter are augmented by the elevated energy levels of the X-ray beam [51]. However, our results accepted our null hypothesis and demonstrated that the change in tube voltage of CBCT did not alter micromorphometric measurements of both trabecular and cortical bones. This finding is consistent with the findings of a previous study, in which the tube voltage had no effect on bone structure assessment. [18] Moreover, previous research has suggested that changing tube potential from 80 to 90 in adult patients can result dose reduction of 19% to 24.6%. [27, 52] Since the change in tube voltage has no effect on micromorphometric measurements of both trabecular and cortical bones, CBCT images obtained at 80 kV may be recommended to evaluate bone structure for implant planning to balance image quality while limiting the dose to the patient.

Many studies have compared the reliability and accuracy of CBCT measurements with those of µCT for the microstructural analysis of alveolar bones. According to the previous results, the two methods exhibited different levels of agreement [15, 40, 53]. Nevertheless, most of these studies have used correlation analysis to show the agreement between the measured variables. However, correlation and agreement are not synonymous. While correlation shows the presence of a relationship between two variables, agreement determines the concordance between two measurements of a single variable [54]. Therefore, the use of Bland–Altman plots providing measurement bias within 95% agreement between two imaging methods is one of the major strengths of this study verifying the accuracy of our findings.

To the best of our knowledge, this is the first study solely comparing the effect of tube potential on the accuracy of morphometric measurements of CBCT and µCT images, including the evaluation of both trabecular and cortical bones. However, a few limitations of the study should be considered before drawing further conclusions. Despite similarities in the trabecular architecture of human and ovine mandibles, the differences in bone density and cortical thickness of the two groups raise questions about the findings' applicability to human mandibles. Therefore, future in vivo human studies are necessary to validate the presented results and their clinical extrapolation. Moreover, although modeling wax and low-density foam boards were used to simulate soft tissue during scanning, it is already known that these do not fully mimic in vivo conditions. It should be noted that the use of simulation materials might cause differences in attenuation and scatter, which may have an impact

on image quality and measurement accuracy. Therefore, the effect of soft tissue, other anatomical structures and any potential movement during scanning were not in consideration resulting in clearer images with fewer artifacts. Furthermore, the measurement outcomes are specific to the CBCT system used in the present study and therefore, it is possible that the results may vary with devices from different manufacturers, models, and voxel resolutions.

It is essential to optimize the exposure protocols by adhering to the ALARA (As Low As Reasonably Achievable) principle, taking all relevant exposure factors into account. Even though the current study evaluated the effect of only tube voltage, our results may provide strong insights for adjusting imaging protocols for trabecular and cortical bone evaluations prior to dental implant surgery. The effect of tube voltage on image quality and radiation dose in CBCT is multifactorial. The optimal tube voltage for CBCT imaging of the hard tissues of the dento-maxillofacial region is still debatable and to some extent, specific for each CBCT device, depending on factors other than total filtration and other sources of noise besides scatter and quantum noise. However, the optimization approach and general findings of this study are universally applicable. [27] The fact that reducing the tube voltage of CBCT has no effect on morphometric measurements may allow us to choose the lowest possible voltage which may further provide advantages such as reduction of x-ray scatter, resulting in higher image quality, thereby enhancing the reliability of bone measurements. However, further clinical validation of the proposed exposure protocol, including the effect of other exposure parameters, is necessary.

Conclusions

Our null hypothesis was accepted since the present findings demonstrated that adjusting the tube voltage from 80 to 90 did not cause any significant change in the measurements of trabecular or cortical bone parameters. Therefore, it may be reasonable to suggest the use of CBCT images obtained with 80 kV for the assessment of bone microstructure before implant surgery and during the bone-healing phase to minimize the dose to the patient without compromising any morphometric measurements. Due to the fact that no difference was found between measurements of μCT and CBCT for BV/TV and Ct.Ar, these parameters may be preferred in clinical settings to evaluate the bone quality using CBCT images to predict long-term implant stability and bone strength after jawbone surgery. Nevertheless, given the limitations of this study and the variability among CBCT systems, future human studies using in vivo images obtained with different CBCT devices are necessary to validate these results.

Acknowledgements

A part of this study was presented as an oral presentation at the 4th International Oral Diagnosis and Maxillofacial Radiology Congress, held on October 19–23, 2024, in Izmir, Turkey. We extend our gratitude to the personnel at Ege University Central Research Test and Analysis Laboratory Application and Research Center (EGEMATAL) (Izmir, Turkey) and the staff of BOYUT Imaging Center (Izmir, Turkey) for their invaluable assistance and support during the image acquisition process for this study.

Authors' contributions

•OB: Obtained the samples, conducted laboratory experiments, performed radiological imaging, organized data sets, contributed to the data interpretation, and critically revised the manuscript. •EÖ: Designed the study, obtained ethical approval and scientific research project authorization, contributed to drafting the manuscript, and provided oversight for the overall research process. •AM: Performed statistical analyses of the data, contributed to the interpretation of the results, and provided feedback on the manuscript. •BGB: Conceived the study, supervised all phases of the research, contributed to the experimental design, provided critical feedback and final approval, contributed to data interpretation, and critically revised the manuscript. •All authors: Read and approved the final manuscript.

Funding

This work was funded by the Ege University Scientific Research Projects Coordination Unit. Project Number: 22767.

Data availability

The datasets generated and analyzed during the current study are not publicly available due to restrictions related to ethical considerations, the proprietary nature of the imaging data, and the context in which the data were collected. However, they are available from the corresponding author upon reasonable request.

Declarations

Ethics approval and consent to participate

This in vitro study did not involve any experiments with live animals or human participants conducted by the authors. All methods were performed in compliance with institutional, national, and international guidelines, including Directive 2010/63/EU on the protection of animals used for scientific purposes. The study protocol was reviewed and approved by the University's Local Ethics Committee for Animal Experiments (protocol no: 2020–034). The committee confirmed that the use of tissues from deceased animals, procured from local meat markets, does not raise ethical concerns and is exempt from requiring additional ethics approval. The fresh animal samples used in this study were obtained from ovine producers as meat products intended for human consumption. No animals were specifically sacrificed for the purposes of this research. Informed consent from owners was not applicable, as the samples were commercially sourced and not traceable to individual ownership.

Competing interests

The authors declare no competing interests.

Received: 20 November 2024 Accepted: 20 March 2025
Published online: 29 April 2025

References

1. de Elío OJ, del Canto DA, del Canto DM, Orea CJ, del Canto PM, Calvo JS. Alveolar Bone Density and Width Affect Primary Implant Stability. Journal of Oral Implantology. 2020;46(4):389–95. https://doi.org/10.1563/aaid-joi-D-19-00028.

2. Fanuscu MI, Chang TL. Three-dimensional morphometric analysis of human cadaver bone: microstructural data from maxilla and mandible. Clin Oral Implants Res. 2004;15(2):213–8. https://doi.org/10.1111/J.1600-0501.2004.00969.X.
3. Sakka S, Coulthard P. Bone quality: a reality for the process of osseointegration. Implant Dent. 2009;18(6):480–5. https://doi.org/10.1097/ID.0B013E3181BB840D.
4. Peev S, Yotsova R, Parushev . Histomorphometric Analysis of Osseointegrated Intraosseous Dental Implants Using Undecalcified Specimens: A Scoping Review. Biomimetics. 2024;9(11):672. https://doi.org/10.3390/biomimetics9110672
5. Kulah K, Gulsahi A, Kamburoğlu K, et al. Evaluation of maxillary trabecular microstructure as an indicator of implant stability by using 2 cone beam computed tomography systems and micro-computed tomography. Oral Surg Oral Med Oral Pathol Oral Radiol. 2019;127(3):247–56. https://doi.org/10.1016/J.OOOO.2018.11.014.
6. Bouxsein ML, Boyd SK, Christiansen BA, Guldberg RE, Jepsen KJ, Müller R. Guidelines for assessment of bone microstructure in rodents using micro-computed tomography. J Bone Miner Res. 2010;25(7):1468–86. https://doi.org/10.1002/JBMR.141.
7. Burghardt AJ, Link TM, Majumdar S. High-resolution computed tomography for clinical imaging of bone microarchitecture. Clin Orthop Relat Res. 2011;469(8):2179–93. https://doi.org/10.1007/S11999-010-1766-X.
8. Ritman EL. Current Status of Developments and Applications of Micro-CT. 2011;13:531–552. https://doi.org/10.1146/annurev-bioeng-071910-124717
9. Lyu HZ, Lee JH. Correlation between two-dimensional micro-CT and histomorphometry for assessment of the implant osseointegration in rabbit tibia model. Biomater Res. 2021;25(1). https://doi.org/10.1186/s40824-021-00213-x
10. Jacobs R, Vranckx M, Vanderstuyft T, Quirynen M, Salmon B. CBCT vs other imaging modalities to assess peri-implant bone and diagnose complications: a systematic review. Eur J Oral Implantol. 2018;11(Suppl 1):77–92.
11. Guha I, Klintström B, Klintström E, et al. A comparative study of trabecular bone micro-structural measurements using different CT modalities. Phys Med Biol. 2020;65(23): 235029. https://doi.org/10.1088/1361-6560/abc367.
12. Ibrahim N, Parsa A, Hassan B, et al. Comparison of anterior and posterior trabecular bone microstructure of human mandible using cone-beam CT and micro CT. BMC Oral Health. 2021;21(1):249. https://doi.org/10.1186/s12903-021-01595-z.
13. Parsa A, Ibrahim N, Hassan B, van der Stelt P, Wismeijer D. Bone quality evaluation at dental implant site using multislice CT, micro-CT, and cone beam CT. Clin Oral Implants Res. 2015;26(1):e1–7. https://doi.org/10.1111/CLR.12315.
14. He RT, Tu MG, Huang HL, Tsai MT, Wu J, Hsu JT. Improving the prediction of the trabecular bone microarchitectural parameters using dental cone-beam computed tomography. BMC Med Imaging. 2019;19(1):10. https://doi.org/10.1186/s12880-019-0313-9.
15. Ibrahim N, Parsa A, Hassan B, van der Stelt P, Aartman IHA, Nambiar P. Influence of object location in different FOVs on trabecular bone microstructure measurements of human mandible: a cone beam CT study. Dentomaxillofacial Radiology. 2014;43(2):20130329. https://doi.org/10.1259/dmfr.20130329.
16. Tayman MA, Kamburoğlu K, Ocak M, Özen D. Effect of different voxel sizes on the accuracy of CBCT measurements of trabecular bone microstructure: A comparative micro-CT study. Imaging Sci Dent. 2022;52(2):171. https://doi.org/10.5624/isd.20220025.
17. Tsai MT, He RT, Huang HL, Tu MG, Hsu JT. Effect of Scanning Resolution on the Prediction of Trabecular Bone Microarchitectures Using Dental Cone Beam Computed Tomography. Diagnostics. 2020;10(6):368. https://doi.org/10.3390/diagnostics10060368.
18. Pauwels R, Faruangsaeng T, Charoenkarn T, Ngonphloy N, Panmekiate S. Effect of exposure parameters and voxel size on bone structure analysis in CBCT. Dentomaxillofacial Radiology. 2015;44(8):20150078. https://doi.org/10.1259/dmfr.20150078.
19. Hsu PY, Tsai MT, Wang SP, Chen YJ, Wu J, Hsu JT. Cortical Bone Morphological and Trabecular Bone Microarchitectural Changes in the Mandible and Femoral Neck of Ovariectomized Rats. PLoS ONE. 2016;11(4): e0154367. https://doi.org/10.1371/journal.pone.0154367.
20. Panmekiate S, Ngonphloy N, Charoenkarn T, Faruangsaeng T, Pauwels R. Comparison of mandibular bone microarchitecture between micro-CT and CBCT images. Dentomaxillofacial Radiology. 2015;44(5):20140322. https://doi.org/10.1259/dmfr.20140322.
21. Doube M, Kłosowski MM, Arganda-Carreras I, et al. BoneJ: Free and extensible bone image analysis in ImageJ. Bone. 2010;47(6):1076–9. https://doi.org/10.1016/j.bone.2010.08.023.
22. Saetang J, Issuriya A, Suyapoh W, Sornying P, Nilsuwan K, Benjakul S. Bio-Calcium from Skipjack Tuna Frame Attenuates Bone Loss in Ovariectomy-Induced Osteoporosis Rats. Mar Drugs. 2024;22(10):472. https://doi.org/10.3390/md22100472.
23. Koo TK, Li MY. A Guideline of Selecting and Reporting Intraclass Correlation Coefficients for Reliability Research. J Chiropr Med. 2016;15(2):155–63. https://doi.org/10.1016/j.jcm.2016.02.012.
24. Boutry N, Cortet B, Dubois P, Marchandise X, Cotten A. Trabecular bone structure of the calcaneus: preliminary in vivo MR imaging assessment in men with osteoporosis. Radiology. 2003;227(3):708–17. https://doi.org/10.1148/RADIOL.2273020420.
25. Bilgili E. Influence of Voxel Size on Evaluation of Trabecular Bone Microstructure on Human Mandibles: A CBCT study. Journal of Basic and Clinical Health Sciences. 2022;6(3):791–7. https://doi.org/10.30621/jbachs.1037333.
26. Anthony Rabba J, Irinam Efenji G, Omachoko Uloko F, et al. Investigation of the optimal tube voltage kV exposure parameters for general X-ray of dental cone-beam computed tomography: A cephalometric view. Advances in Radiotherapy & Nuclear Medicine. 2024;2(2):2972. https://doi.org/10.36922/arnm.2972.
27. Pauwels R, Silkosessak O, Jacobs R, Bogaerts R, Bosmans H, Panmekiate S. A pragmatic approach to determine the optimal kVp in cone beam CT: balancing contrast-to-noise ratio and radiation dose. Dentomaxillofacial Radiology. 2014;43. https://doi.org/10.1259/dmfr.20140059
28. Kaasalainen T, Ekholm M, Siiskonen T, Kortesniemi M. Dental cone beam CT: An updated review. Physica Med. 2021;88:193–217. https://doi.org/10.1016/j.ejmp.2021.07.007.
29. Szabelska A, Tatara MR, Krupski W. Morphological, densitometric and mechanical properties of mandible in 5-month-old Polish Merino sheep. BMC Vet Res. 2016;13(1):12. https://doi.org/10.1186/s12917-016-0921-3.
30. Veigel E, Moore RJ, Zarrinkalam MR, et al. Osteopenia in the maxillofacial area: a study in sheep. Osteoporos Int. 2011;22(4):1115–21. https://doi.org/10.1007/s00198-010-1289-z.
31. Dias IR, Camassa JA, Bordelo JA, et al. Preclinical and Translational Studies in Small Ruminants (Sheep and Goat) as Models for Osteoporosis Research. Curr Osteoporos Rep. 2018;16(2):182–97. https://doi.org/10.1007/s11914-018-0431-2.
32. Pearce A, Richards R, Milz S, Schneider E, Pearce S. Animal models for implant biomaterial research in bone: A review. Eur Cell Mater. 2007;13:1–10. https://doi.org/10.22203/eCM.v013a01.
33. Watson PJ, Fitton LC, Meloro C, Fagan MJ, Gröning F. Mechanical adaptation of trabecular bone morphology in the mammalian mandible. Sci Rep. 2018;8(1):7277. https://doi.org/10.1038/s41598-018-25597-0.
34. den Boer FC, Patka P, Bakker FC, et al. New segmental long bone defect model in sheep: Quantitative analysis of healing with dual energy X-ray absorptiometry. J Orthop Res. 1999;17(5):654–60. https://doi.org/10.1002/jor.1100170506.
35. Cabrera D, Kruger M, Wolber FM, Roy NC, Fraser K. Effects of short- and long-term glucocorticoid-induced osteoporosis on plasma metabolome and lipidome of ovariectomized sheep. BMC Musculoskelet Disord. 2020;21(1):349. https://doi.org/10.1186/s12891-020-03362-7.
36. Coelho CA, Bordelo JP, Camassa JA, et al. Evaluation of hematology, general serum biochemistry, bone turnover markers and bone marrow cytology in a glucocorticoid treated ovariectomized sheep model for osteoporosis research. An Acad Bras Cienc. 2020;92(4). https://doi.org/10.1590/0001-3765202020200435
37. Waarsing JH, Day JS, Weinans H. An Improved Segmentation Method for In Vivo µCT Imaging. J Bone Miner Res. 2004;19(10):1640–50. https://doi.org/10.1359/JBMR.040705.
38. Alomari AH, Wille ML, Langton CM. Bone volume fraction and structural parameters for estimation of mechanical stiffness and failure load of human cancellous bone samples; in-vitro comparison of ultrasound transit time spectroscopy and X-ray µCT. Bone. 2018;107:145–53. https://doi.org/10.1016/j.bone.2017.11.021.

39. Tabarany K, Aboulfotouh M, Ashmawy M. Validity of cone beam computed tomography voxel density values: a review. Int J Adv Res (Indore). 2018;6(9):103–21. https://doi.org/10.21474/IJAR01/7650.
40. Ibrahim N, Parsa A, Hassan B, van der Stelt P, Aartman IHA, Wismeijer D. Accuracy of trabecular bone microstructural measurement at planned dental implant sites using cone-beam <scp>CT</scp> datasets. Clin Oral Implants Res. 2014;25(8):941–5. https://doi.org/10.1111/clr.12163.
41. de Oliveira RC, Leles CR, Lindh C, Ribeiro-Rotta RF. Bone tissue microarchitectural characteristics at dental implant sites. Part 1: identification of clinical-related parameters. Clin Oral Implants Res. 2012;23(8):981–6. https://doi.org/10.1111/J.1600-0501.2011.02243.X.
42. Issever AS, Link TM, Kentenich M, et al. Assessment of trabecular bone structure using MDCT: comparison of 64- and 320-slice CT using HR-pQCT as the reference standard. Eur Radiol. 2010;20(2):458–68. https://doi.org/10.1007/S00330-009-1571-7.
43. Van Dessel J, Huang Y, Depypere M, Rubira-Bullen I, Maes F, Jacobs R. A comparative evaluation of cone beam CT and micro-CT on trabecular bone structures in the human mandible. Dentomaxillofacial Radiology. 2013;42(8):20130145. https://doi.org/10.1259/dmfr.20130145.
44. Adams JE. Quantitative computed tomography. Eur J Radiol. 2009;71(3):415–24. https://doi.org/10.1016/j.ejrad.2009.04.074.
45. Ho JT, Wu J, Huang HL, Chen MY, Fuh LJ, Hsu JT. Trabecular bone structural parameters evaluated using dental cone-beam computed tomography: cellular synthetic bones. Biomed Eng Online. 2013;12(1):115. https://doi.org/10.1186/1475-925X-12-115.
46. Bechara B, McMahan CA, Moore WS, Noujeim M, Geha H, Teixeira FB. Contrast-to-noise ratio difference in small field of view cone beam computed tomography machines. J Oral Sci. 2012;54(3):227–32. https://doi.org/10.2334/josnusd.54.227.
47. Schulze R, Heil U, Groß D, et al. Artefacts in CBCT: a review. Dentomaxillofac Radiol. 2011;40(5):265–73. https://doi.org/10.1259/DMFR/30642039.
48. Maret D, Peters OA, Galibourg A, et al. Comparison of the Accuracy of 3-dimensional Cone-beam Computed Tomography and Micro-Computed Tomography Reconstructions by Using Different Voxel Sizes. J Endod. 2014;40(9):1321–6. https://doi.org/10.1016/j.joen.2014.04.014.
49. Maret D, Telmon N, Peters OA, et al. Effect of voxel size on the accuracy of 3D reconstructions with cone beam CT. Dentomaxillofacial Radiology. 2012;41(8):649–55. https://doi.org/10.1259/dmfr/81804525.
50. Sugiura T, Yamamoto K, Horita S, Murakami K, Tsutsumi S, Kirita T. The effects of bone density and crestal cortical bone thickness on micromotion and peri-implant bone strain distribution in an immediately loaded implant: a nonlinear finite element analysis. J Periodontal Implant Sci. 2016;46(3):152–65. https://doi.org/10.5051/jpis.2016.46.3.152.
51. Freitas DQ, Fontenele RC, Nascimento EHL, Vasconcelos TV, Noujeim M. Influence of acquisition parameters on the magnitude of cone beam computed tomography artifacts. Dentomaxillofacial Radiology. 2018;47(8):20180151. https://doi.org/10.1259/dmfr.20180151.
52. Pauwels R, Jacobs R, Bogaerts R, Bosmans H, Panmekiate S. Determination of size-specific exposure settings in dental cone-beam CT. Eur Radiol. 2017;27(1):279–85. https://doi.org/10.1007/s00330-016-4353-z.
53. Van Dessel J, Nicolielo LFP, Huang Y, et al. Accuracy and reliability of different cone beam computed tomography (CBCT) devices for structural analysis of alveolar bone in comparison with multislice CT and micro-CT. Eur J Oral Implantol. 2017;10(1):95–105.
54. Ranganathan P, Pramesh C, Aggarwal R. Common pitfalls in statistical analysis: Measures of agreement. Perspect Clin Res. 2017;8(4):187. https://doi.org/10.4103/picr.PICR_123_17.

Publisher's Note